Journal of Applied Fluid Mechanics, Vol. 10, No. 5, pp. 1441-1449, 2017.
Available online at www.jafmonline.net, ISSN 1735-3572, EISSN 1735-3645.
DOI: 10.18869/acadpub.jafm.73.242.26983

Dynamic Simulation in Guide Vane Opening Process of a Pump-Turbine in Pump Mode

L. Han[1], H. J. Wang[1†], Y. H. Gao[1], D. Y. Li[1], R. Z. Gong[1] and X. Z. Wei[2]

[1] *School of Energy Science and Engineering, Harbin Institute of Technology, Harbin 150001, China*
[2] *State Key Laboratory of Hydro-Power Equipment, Harbin Institute of Large Electrical Machinery, Harbin 150040, China*

†*Corresponding Author Email: wanghongjie@hit.edu.cn*

(Received July 23, 2016; accepted May 10, 2017)

ABSTRACT

During the process of switching conditions in pump-turbine, unstable flow would take place and seriously impact on the stability and safety. This paper deals with the guide vanes' moving process in pump mode through unsteady numerical simulations. Dynamic mesh methodology is used for simulations in which GVO (Guide Vane Opening) from 9mm to 26mm. Simulation results approve that, there are many complex vortex structures and flow blockages phenomena under small GVO condition. Through the mathematical method of Fast Fourier Transform (FFT) and Short-Time Fourier Transform (STFT), the dominant pressure fluctuation frequencies are from runner blade passing frequency (BPF) and its harmonic frequency, as well as some other low frequencies are from unsteady flow states. Furthermore, the flow states are more unstable and complex under small guide vanes moving process. Compared with fixed GVO position, the flow states are more unstable and complex under guide vanes moving process, while the amplitude of main frequencies becomes higher.

Keywords: Pump turbine; Pressure fluctuation; Dynamic mesh; Guide vane opening.

NOMENCLATURE

$\vec{A}_j$	area vector	$\vec{u}_g$	mesh moving velocity
f_n	rotation frequency	$\vec{u}$	velocity vector
GVO	guide vqne opening	V(t)	controlling volume
H	hydraulic head		
k	kinetic energy	ε	energy dissipation rate
Q	discharge	ν	specific speed
t	time	τ	shear stress

1. INTRODUCTION

Solar and wind, typical renewable energies, are examples of intermittent energy sources and may cause unstable operation of the power grid (Trivedi *et al*. 2013). Hence, pumped storage power plants (PSPP) are widely believed as having great potential in storing large amounts of electrical energy and adjusting the variations. Li *et al*. (2015 a) and Li *et al*. (2015 b) carried out lots of studies in pump mode of a pump-turbine. They analyzed flow characteristics, especially in hump regions for a given guide vane setting and different guide vane opening. Especially, Li *et al*. (2015 c) and Wang *et al*. (2015) simulated the pressure fluctuation in pump turbine with dynamic mesh technology. However, these achievements were obtained based on constant guide vane opening. For frequently switching between the pump mode and turbine mode, it is necessary to understand the guide opening and closing process in both modes. Rodriguez (2007) proves that highest vibration levels in pump-turbines are originated in the rotor stator interaction which is called RSI. This phenomenon is also stated by Qian and Arakawa (2010). Furthermore, it possibly causes fatigue failure, if the runner was designed without proper consideration on its dynamic behavior (Tanaka (2011), Egusquiza *et al*. (2002)). Ciocan and Kueny (2006) has done an exhaustive experimental exploration of the flow and pressure fields between runner and guide vanes of a pump-turbine using LDV, PIV and an unsteady 5 sensors probe for design and off-design conditions. Guo *et al*. (2014)

states that the amplitude of the pressure fluctuation decreases with the increase of the distance to runner. Secondly, experimental measurements and numerical simulations on pressure fluctuation have been also carried out to investigate the causes of instabilities in the vaneless region. Houde *et al*. (2012b) and Houde *et al*. (2012a) have measured the pressure fluctuations on a wide band of frequencies, both in a blade-to-blade channel and on the pressure and suction side of the same blade. It has been observed that the pressure fluctuation amplitude during transient operating conditions is higher than that during steady state operations. Ciocan *et al*. (2000) introduced optical experimental techniques, LDV and PIV, allowing an access to the unsteady 3D velocity field in real configuration of hydraulic test models. A detailed experimental analysis of the unsteady flow in turbo-machinery was made with a five sensors unsteady total pressure probe and validated by comparison with LDV measurements in a pump-turbine model (Ciocan and Kueny 2006). Ran *et al*. (2012) tested pressure fluctuation characteristics and obtained the amplitudes of the pressure fluctuations at large partial flow conditions near the first positive slope are much larger than those at stable operating conditions.

Hasmatuchi *et al*. (2011) solved incompressible unsteady Reynolds-Averaged Navier-Stokes equations and compared with experiment at the best efficiency point, runaway and braking operating conditions. It appears a 0.7 fn rotating stall in the vaneless region. Zobeiri *et al*. (2006) preformed RANS simulations in a reduced-scale model of a ν = 0.19 specific speed pump-turbine strong influence of the potential effect in the interactions between the guide vanes and the rotating impeller blades. Sun *et al*. (2012) shows that pressure fluctuations in design opening angle were much lower than those in off design opening angle through SST k − ω turbulence model. The simulation results have also confirmed the results gained in model tests. Yin (2011) showed that the DES method is adapted to capture the pressure fluctuation characteristics and suggested that low frequency pressure fluctuations (f /9 fn = 11.27%) are remarkable. Although many different turbulent models are performed by different researchers, it still lacks to assess the accuracy. Furthermore, the transient process of the pump-turbines should be also focused. All the studies above are focused on constant GVO conditions. Rare research is conducted for a pump-turbine on transient simulation of pump-turbine. Fortunately, there are some researches which concern about the transient process for pump. Experiments conducted by (Thanapandi and Prasad 1995) showed that pump behavior was disturbed during startup and stopping process. Li *et al*. (2010) uses DSR (Dynamic Slip Region) method which are fully dynamic, closer to reality, and capable of capturing the instantaneous impeller-volute interactions. Gao *et al*. (2013) has simulated the transient performance of the reactor coolant pump which has an excellent agreement with the Tsukamoto's experimental results. Wu *et al*. (2010) simulated the transient characteristics during the valve's opening process and concludes that the Q/H curve deviates from the steady-state value. Actually, pump-turbine switches frequently between the pump mode and the turbine mode. Pressure fluctuation appears during the process, through the flow parts including the runner, guide vanes and vaneless region, etc. Hence, in this paper, we will perform 3D unsteady simulations using the dynamic mesh to investigate pressure fluctuation in guide vane and vaneless region as the guide vanes open from guide vanes opening (GVO) equal to 9mm to GVO equal to 26mm. The pressure fluctuation will be observed in the dynamic process of the GVO movement. With this process, more flow phenomena will be found and the frequencies and amplitudes of the pressure fluctuation in the vaneless and distribution region are strongly enhanced which cannot be observed in the simulation without GVO movement.

2. CASE STUDY

2.1 Modelling

The structure parameters of the hydraulic turbine are listed in Tab.1 which was tested in State Key Laboratory of Hydro-Power Equipment. The simulation ranges through the whole pump-turbine from inlet to outlet, including draft tube, runner, guide vanes, stay vanes and spiral casing in flow order. The model is built with UG NX software. According to the parameters in Tab.1, one firstly builds the machinery part and then uses the bool subtract method to obtain the flow region.

Table 1 Basic structure parameters of the pump-turbine model

Parameters	Values
Number of runner blades	9
Number of guide vanes	20
Number of stay vanes	20
Outlet diameter of the runner	524mm
Inlet diameter of the runner	274mm
Distribution diameter of guide vanes	634mm
Inlet diameter of the spiral casing	280.5mm
Outlet diameter of the draft tube	560.95mm

2.2 Turbulent Model

Wilcox (2006) has reviewed the turbulent model and indicated the advantages of each turbulent model. Launder and Spalding (1972) indicated that there are two turbulent models named Reynolds stress model and eddy viscosity model. In this paper, one uses the second one to solve the N-S equation with assumption that Reynolds Stress can be replaced by mean velocity gradient as written in Eq.1:

$$T=-\rho\ \overline{u_i'u_j'} =\rho\ \nu_t\left(\frac{\partial \overline{u_i}}{\partial x_j}+\frac{\partial \overline{u_j}}{\partial x_i}\right)-\frac{2}{3}\rho\left(k+\nu_t\frac{\partial \overline{u_i}}{\partial x_i}\right)\sigma_{ij} \quad (1)$$

Actually, this paper uses the two-equation model named RNG k − ε model. This method was first proposed by Kollmann and Dynamics (1980). Meanwhile, this model includes viscosity analytical formulae in low Re condition. Hence, in code Fluent, one chooses the RNG k−ε model accompanied by wall function. Secondly, for solving the finite equations, this paper uses finite volume method (Second Order Upwind) to discrete the N-S equations. SIMPLEC (SIMPLE-Consistent) algorithm which belongs to Segregated Solution Method is chosen. In present, structured mesh has advantages in convergence and precision while unstructured mesh can persuade complex geometry problem. In this case, considering guide vanes rotating in the calculation, unstructured mesh is used in the guide vanes moving region. In the other regions, structured mesh is applied.

2.3 The Validation of the Simulation

In this paper, 6 different mesh were taken into calculation and compared with the experience. Head and torque are calculated with different meshes. For the model turbine working condition, the head is chosen as 30m and speed of rotation is 1000rpm. Obviously, As the quantity increases, the head and torque become steady. Meanwhile, the results from simulations are not far from the experiments which confirm the accuracy of simulations in this paper.

3. PRESSURE FLUCTUATION ANALYSE OF FLOW CHARACTERISTICS IN PUMP MODE

For pump-turbine, stability is influenced by dynamic vortex and also negative flow. In this section, the research focuses on the flow characteristics in different guide vanes opening conditions including 13mm, 19mm and 25mm. GVO is defined as the throat in a 2D design of the guide vane. Rotation rate is designed as 1000rpm so the rotating period is 0.06s. An implicit unsteady solver is chosen which time step is 0.0002s. Considering the instability in beginning of the calculation, this paper analyses the time between 0.18s to 1.4s.

In order to visualize the pressure fluctuation, one located 69 points for monitoring. These points include: 8 in spiral casing, 19 in stay vanes, 34 in distribution region, 4 in guide vanes, 4 in draft tube. In this paper, one will focus on the pressure fluctuation in the region of distribution and vaneless as shown in Fig. 2(a).

In Fig. 2(b), ΔH/H presents values which the pressure fluctuation compared with the head. x axis presents the angle along the circumference from 0 to 360◦. Angle between the adjacent peak point and valley in the figure is about 18◦, corresponding to the installation angle which is also 18◦. In three GVO conditions, Fast Fourier Transform is used to analyze the spectrum characteristic. Fig.3 shows the information for 4 points in vaneless region. They are VL01, VL13, VL20, VL30. Firstly, it is clear that all of the points have the same preliminary peak at 9 fn which fn presents the rotating frequency. Furthermore, 18 fn is larger than 27 fn. 36 fn is nearly 0 compared with the others. Secondly, as the opening turns larger, amplitude of 9 fn turns higher. For point VL1, 9 fn in 25mm is 8158.04Pa, while in 19mm is 6703.80Pa and in 13mm is 5129.24Pa. The amplitudes of frequency at 9 fn, 17 fn, 27 fn, 36 fn increase as the guide vanes open. In 13mm condition, frequency below 5 fn is complex as shown in Fig.3. In the other two opening conditions, this phenomenon disappears, for example in 25 mm condition, the amplitude below 5 fn is near zero. Hence, one can conclude that the process of opening guide vanes is the major reason which produces the pressure fluctuation with low frequency.

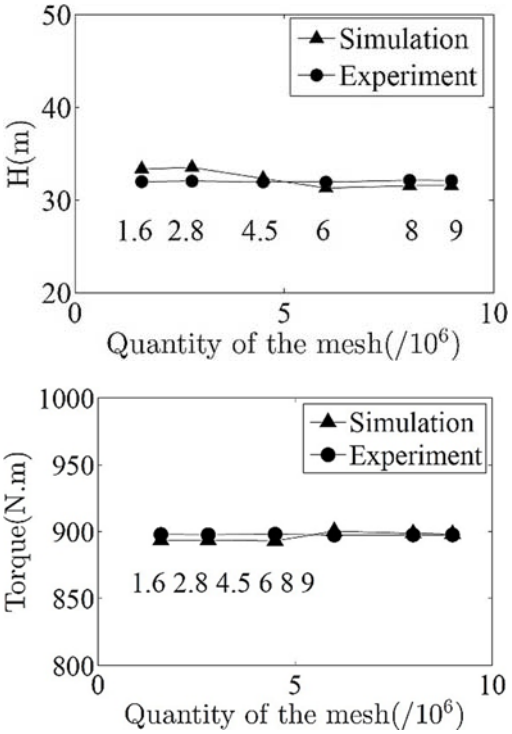

Fig. 1. Comparison between simulations and experiments with different quantities of mesh. Note that: left figure presents the head with function of mesh; Right one presents the torque with function of mesh.

It is proved that the pressure differs periodically along circumference. In order to analyse the flow in distributor clearly, one chooses two positions, SV2 and SV3 near the tongue. And two positions SV10 and SV11 which are 180◦ from SV2. Meanwhile, SV2 and SV10 locate near the outlet of stay vanes while the other two locate near the inlet of stay vanes. FFT is used to analyse these points as shown in Fig. 4. 9 fn and 18 fn are two major frequencies. Obviously, in different opening positions, the magnitude does not change much. For low frequency part, as the opening turns larger, the fluctuation decreases. For 25mm condition, the low frequency

fluctuation nearly disappears. Hence, high frequency fluctuation is not influenced by the opening status and low frequency fluctuation is related to the negative flow in distributor in small GVO condition.

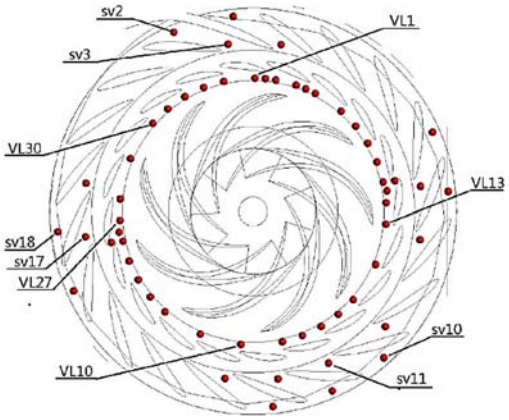

Fig. 2. Monitor points location and the pressure fluctuation in vaneless region.

4. DYNAMIC CHARACTERISTIC WITH DYNAMIC MESH TECHNOLOGY

4.1 Dynamic Mesh Technology

Opening process of a pump-turbine is extremely important for hydraulic engineering which influences the stability of the machine. So, one uses the commercial code ANSYS Fluent to provide the dynamic mesh method. In the calculation, the integral transport equation for an general scalar φ can be expressed as below

$$\frac{d}{dt}\int_v \rho\varphi dv + \int_{\partial v}\rho\varphi\left(\vec{u}-\overrightarrow{u_g}\right).d\vec{A} = \int_{\partial v}\nabla\varphi.d\vec{A} + \int_{\partial v} S_\varphi.dv \quad (2)$$

where, V(t) is the controlling volume in space which varies with time(t); is the velocity vector of fluid; g means the mesh moving velocity; Γ means the diffusivities of the scalar φ and Sφ gives the source term for φ. Using one order finite method for total derivative term in Eq.2,

$$\frac{d}{dt}\int_v \rho\varphi dv = \frac{(\rho\varphi v)^{n+1}-(\rho\varphi v)^n}{\Delta t} \quad (3)$$

in which, n and n + 1 represent the present time and next time step. The controlling volume Vn+1 in (n + 1) time can be written as:

$$V^{n+1} = V^n + \frac{dV}{dt}\Delta t \quad (4)$$

in which dV/dt is the total derivative of controlling volume and can be expressed as:

$$\frac{dV}{dt} = \int_{\partial v}\overrightarrow{u_g}.d\vec{A} = \sum_j^{n_f}\overrightarrow{u_{g.j}}.\overrightarrow{A_j} \quad (5)$$

in which, nf is the totality of the mesh, $\overline{A}_j$ is area vector in plane j. Each element in the right of the Eq.5 can be written as:

$$\overrightarrow{u_g}.\overrightarrow{A_j} = \frac{\delta V_j}{\Delta t} \quad (6)$$

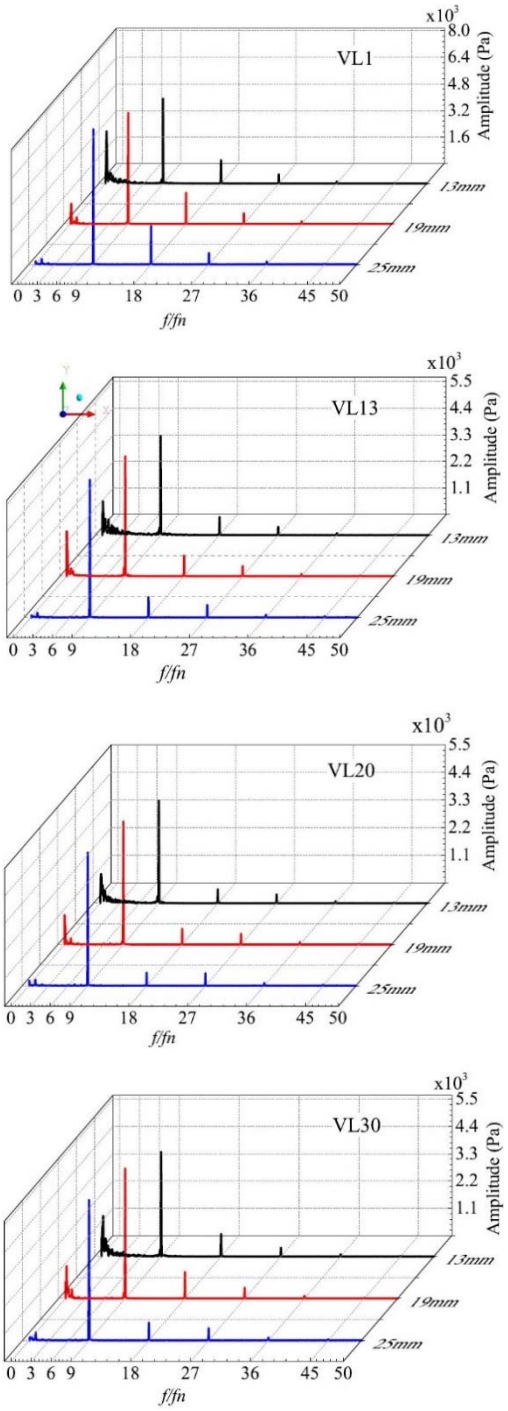

Fig. 3. Spectra comparison among 3 GVO conditions in vaneless region for 4 different monitoring points.

where δVj presents the volume produced by the plane j on the controlling surface in Δt. For simulating the dynamic characteristic of the guide vanes.

4.2 Simulation Strategy

In this paper, Spring Smoothing and Remeshing method is combined to construct dynamic mesh. Association of the two methods can produce triangular prism and tetrahedron meshes. It is easy for triangular prism mesh to be remeshed and

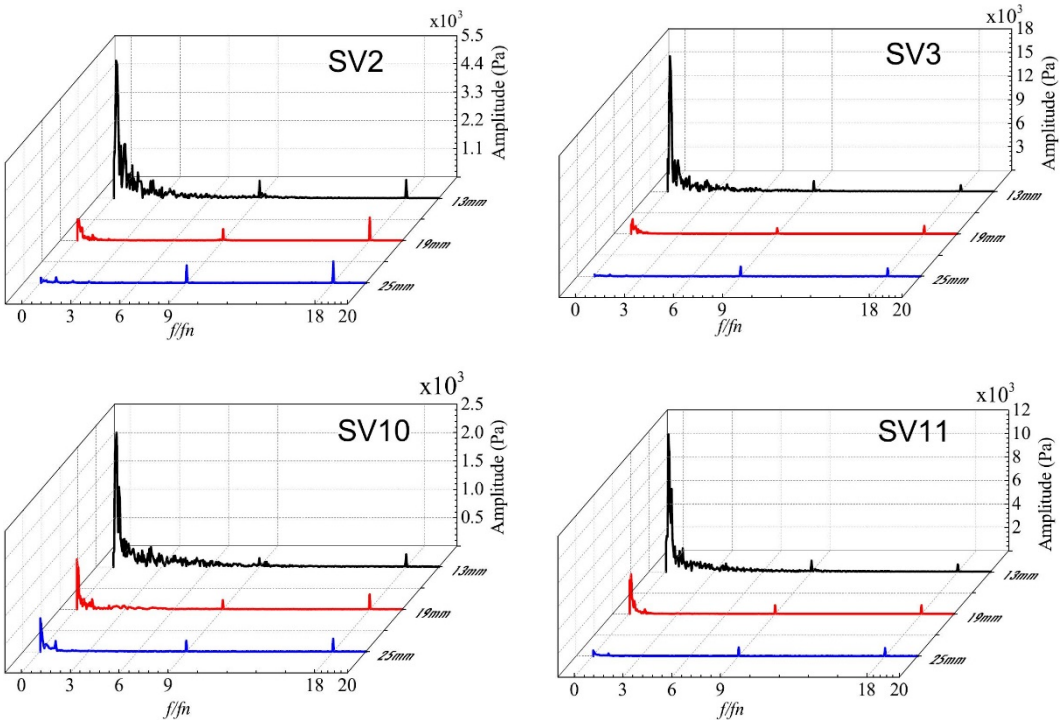

Fig. 4. Spectra comparison among 3 GVO conditions in distributor region for 4 different monitoring points.

improve the construction efficiency. During the simulating process, mesh skewness is below 0.75 which can guarantee enough calculation precision. This paper simulates the opening process of guide vanes from 9mm to 26mm. All the opening parameters are listed in Tab.2. The simulating conditions are remained the same with the simulation above.

Table 2 Guide vane opening regular of guide vanes

Time(s)	Palstance (rad/s)	Guide vane opening (mm)
0~0.3	0	9
0.3~1.08	0.2424	9~26
1.08~1.2	0	26

4.3 Vortex Dynamic

Distributor region is the key part which produces negative flow and pressure fluctuation. This section will analyse the vortex structure calculated by moving guide vanes (first row in Fig.5) comparing with statistic guide vanes (second row in Fig.5). For the fixed GVO conditions, 19mm GVO condition is the best efficiency point as designing which has the most smooth flow in the cascade. This is also observed in dynamic process. Comparing the same GVO condition with, evidently, in the 13mm condition, the dynamic vortex energy is much higher than statistic one. The flow separation near guide vanes appears more strongly than statistic one. At the same time, the intensity of vortex presenting total energy is large in the vaneless region. The vortex is mainly composed by small and smash vortex and the quantity decreases between guide vanes and stay vanes. In 19mm condition, the diversity of the vortex energy in distributor is smaller than that in 13mm. As the GVO changes, the best efficiency surely have shift to another point nearby. Hence, the vortex structure shows a little stronger in dynamic process is reasonable. Hence, the vortex structure appears much messier than statistic simulation. When the opening arrives at 25mm, the difference between dynamic and statistic dis-appears. Furthermore, one can conclude that the moving guide vanes simulation is useful and important for analyzing the vortex structure and so for analyzing the stability of a pump-turbine. In the next section, pressure fluctuation will be studied to understand the instability phenomena deeply.

4.4 Pressure Fluctuation

This section will focus the pressure fluctuation in vaneless and distributor region. The monitoring points VL1, VL13, VL20 and VL30 are chosen in Section 3.

In order to research the effect of the runner rotating accurately, Short-Time Fourier Transform (STFT) is applied here to show how the spectral contents vary as a function of time. Although the STFT has a fixed frequency resolution for all frequencies once the size of the window is chosen, it enables an easier interpretation in terms of harmonics (Gu and Bollen 2000). The STFT analysis for vaneless region is shown in Fig.6.

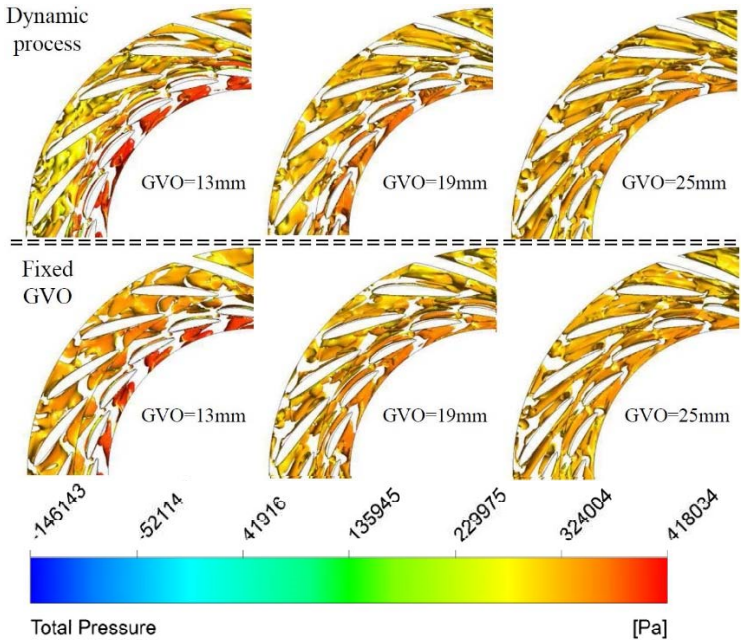

Fig. 5. Comparison of dynamic vortex structure in distributor region at three GVO conditions.

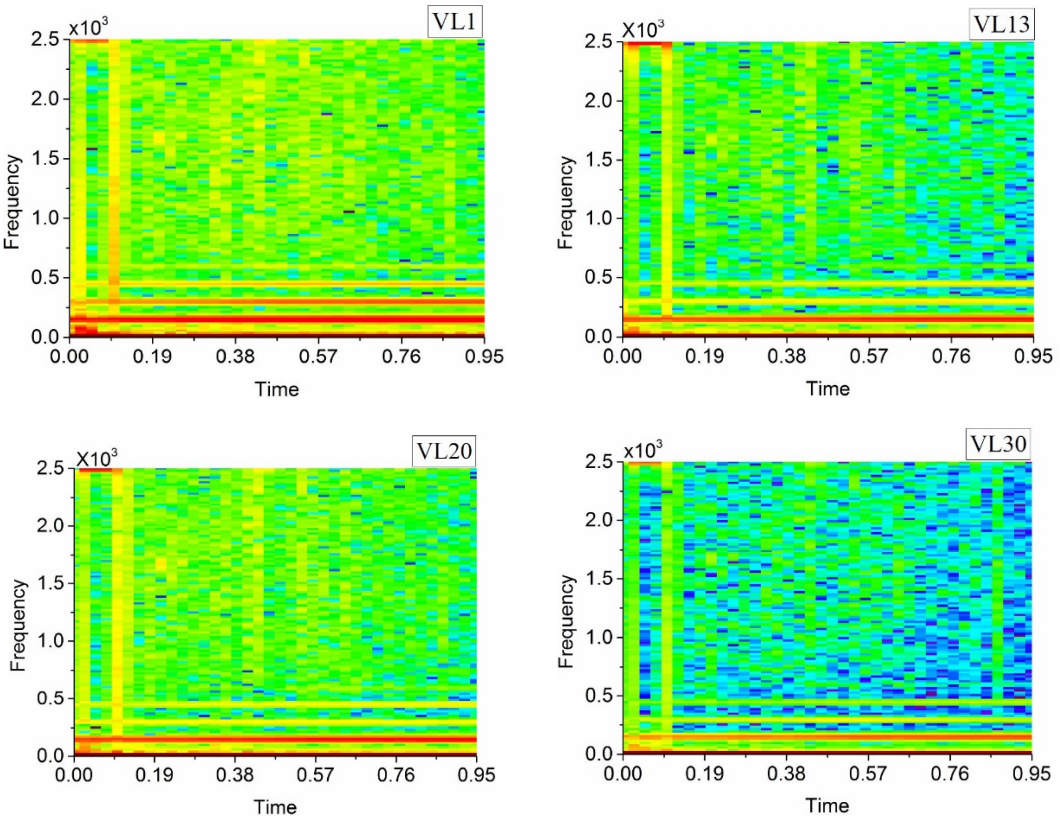

Fig. 6. STFT analyse in vaneless region for four monitoring points.

- For the four monitoring points, 150Hz, 300Hz and 450Hz are evidently high which correspond to 9 fn, 18 fn and 27 fn. Furthermore, 9 fn is more intense than the other two conditions and has larger frequency range. Meanwhile, four monitoring points have low frequency through the whole time range below 10Hz.
- Between 0s and 0.12s, 2500Hz component appears for four monitoring points. This can be related to flow block of small GVO condition.

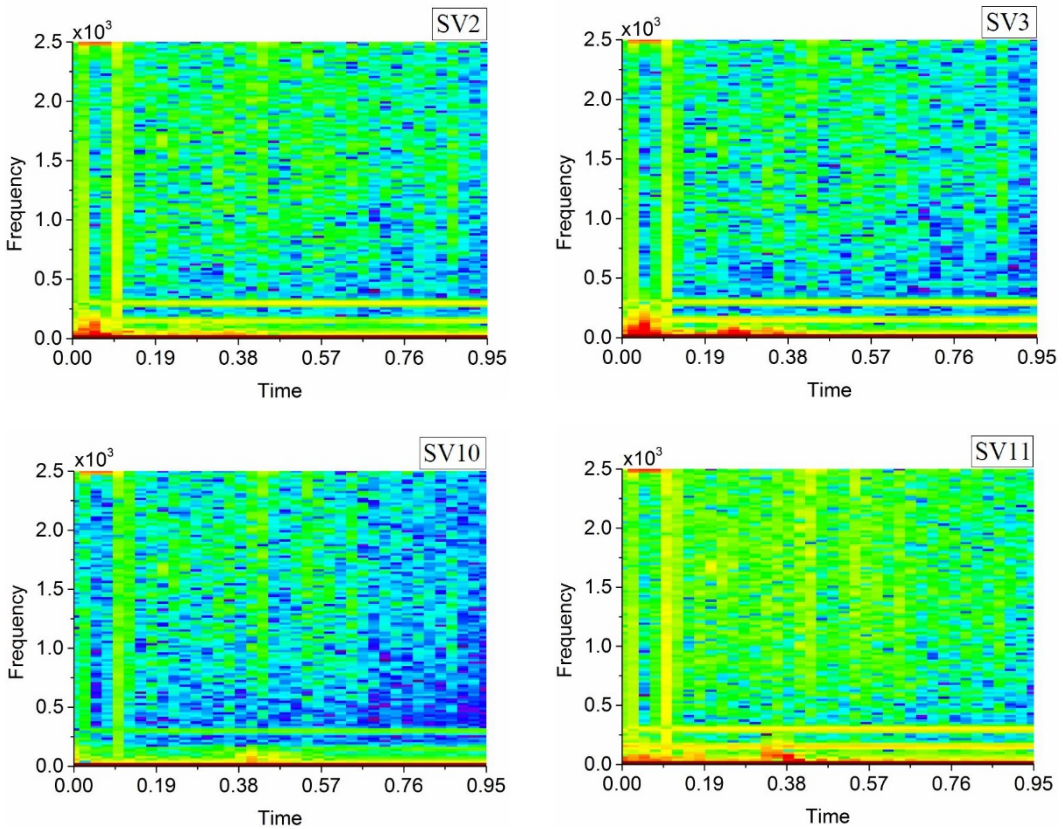

Fig. 7. STFT analyse in distributor region for four monitoring points.

- VL1 and VL20 have different characteristics with VL13 and VL30. VL1 locates near the tongue and VL20 locate opposite to VL1. These two points have clear and intense frequency at 9 fn, 18 fn, 27 fn and even 36 fn. However, the other two points have worn magnitude and much narrower frequency width. 27 fn and 36 fn are nearly disappeared.

Based on analysis above, flow in distribution region comes from the runner region, so it is effected by rotation theoretically. One chose 4 monitoring points as section 3.. Fig.7 illustrates the spectrum information for them. In the whole time period, low frequency, 9 fn and 18 fn have higher amplitude than other frequencies. As 0.12s is the start time of the guide vanes, the amplitude between 0 and 0.12s is about 2500Hz and much higher than fn. This is corresponded to the results without guide vanes moving. But there is still some different phenomena in Fig.6 in vaneless region, the four monitoring points show a concentrated fluctuation region in the beginning of guide vanes opening process. For SV2, this region exists between t=0 and t=0.08 with frequency reaching to 150Hz(9 fn). For SV3, this region extends to 0.38s and the maximum frequency is about 300Hz (18 fn). For SV10, this region is smaller than the other three points and furthermore, the maximum appears at 0.38s. SV11 has the same trend as SV10 but has higher amplitude of 150Hz (9 fn). These results claim that the process of guide vanes opening effects 9 fn and 18 fn, especially for the point near the tongue. Moreover, the high fluctuation regions locate before t=0.38s, which says that with the guide vanes opening from 9mm to 13mm, negative flow and unsteady phenomena appear in the distributor region.

Comparing the results as guide vanes open with the results in section3., the low frequency pressure fluctuation is higher; the 9 fn and 18 fn are relatively smaller.

5. CONCLUSION

3D unsteady simulations were preformed in a pump-turbine under pump condition with GVO changing from 13mm to 26mm. For understanding dynamic flow characteristics, dynamic mesh technology is realized within ANSYS code. Through analyzing the vortex dynamic phenomena and pressure fluctuations in vaneless and distributor region, one concludes the influence of guide vanes in the transient processing as following:

(1) For fixed GVO, 13mm condition shows the worst flow phenomena. There are flow blockage and complex vortex structure in two regions. In GVO 19mm and 25mm conditions, as the GVO increases, the flow in vaneless region becomes more stable and smoother. FFT was performed for pressure fluctuation analysis. In GVO 13mm condition, the peak fluctuation is mainly caused by the rotor stator interaction of the runner and

its harmonic frequency 9 fn, 18 fn and 27 fn. As the GVO increases, low frequency decreases respectively and disappeared in 25mm GVO condition.

(2) For simulating the dynamic process within guide vanes opening, guide vanes open from 9mm to 26mm with uniform velocity 0.2424 rad/s. it is obvious that in 13mm position, flow in vaneless and distributor region is more complex and have more vortices with high amplitude. When guide vanes open to 25mm, the statistic and the dynamic results reveal coherence and similar. Hence, the dynamic process enhances the unsteady phenomena to the hydraulic turbine. Meanwhile, analyzing the pressure fluctuation with GVO movement is necessary and useful in simulation. The transient characteristics will be observed.

(3) STFT method were performed during analyzing the pressure fluctuation and proved to be effective. The frequency composes low frequency, coming from the GVO moving and negative flow, and 9 fn, 18 fn and 27 fn which are produced by RSI and harmonic frequency. Comparing with the fixed GVO condition, amplitude of low frequency component is obviously higher. Contrarily, amplitudes at 9 fn and 18 fn are relatively weaker.

Consequently, GVO movement strongly enhances the frequencies and amplitudes of the pressure fluctuation in the vaneless and distribution region. It is necessary to discuss the GVO moving process in the pump-turbine study, furthermore with the pump system influence.

ACKNOWLEDGEMENT

This work was supported by “the Fundamental Research Funds for the Central Universities” (Grant No. HIT. NSRIF2017044).

REFERENCES

Ciocan, G. D. and J. Kueny (2006). Experimental analysis of rotor stator interaction in a pump-turbine. In Proc. *XXIII IAHR Symposium on Hydraulic Machinery and Systems*, Yokohama, Japan.

Ciocan, G. D., A. Franois and J. Kueny (2000). Optical Measurement Techniques for Experimental Analysis of Hydraulic Turbines Rotor - Stator Interaction. In Proceedings of the *ASME Fluids Engineering Division Summer Meeting*, Boston, Massachusetts, USA, June 11-15. Using Smart Source Parsing 11-15 3.

Egusquiza, E., B. Mateos and X. Escaler (2002). Analysis of rotor-stator interaction in operating pump-turbines. In Proceedings of *the XXI IAHR Symposium on Hydraulic Machinery and Systems.*

Gao, H., F. Gao, X. Zhao, J. Chen and X. Cao (2013). Analysis of reactor coolant pump transient performance in primary coolant system during start-up period. *Annals of Nuclear Energy 54*, 202–208.

Gu, Y. and M. Bollen (2000). Time- frequency and time-scale domain analysis of voltage disturbances. Power Delivery, IEEE Transactions on 15(4), 1279–1284.

Guo, L., J. T. Liu, L. Q. Wang, D. Q. Qin and X. Z. Wei (2014). Pressure fluctuation propagation of a pump turbine at pump mode under low head condition. Science China *Technological Sciences 57*(4), 811–818.

Hasmatuchi, V., S. Roth, F. Botero, M. Farhat and F. Avellan (2011). Hydrodynamics of a pump-turbine at off-design operating conditions: Numerical simulation. In Proceedings of *ASME-JSME-KSME Joint Fluids Engineering Conference* 495–506.

Houde, S., R. Fraser, G. Ciocan and C. Deschеˆnes (2012a). Experimental study of the pressure fluctuations on propeller turbine runner blades: part 2, transient conditions. In *IOP Conference Series: Earth and Environmental Science 15*, 062061.

Houde, S., R. Fraser, G. Ciocan and C. Deschеˆnes (2012b). Part 1–experimental study of the pressure fluctuations on propeller turbine runner blades during steady-state operation. In *IOP Conference Series: Earth and Environmental Science 15*, 022004.

Kollmann, W. and V. K. I. F. F. Dynamics (1980). Prediction methods for turbulent flows. *Hemisphere Pub. Corp*.

Launder, B. E. and D. B. Spalding (1972). Lectures in mathematical models of turbulence. *Von Karman Institute for Fluid Dynamics*.

Li, D. Y., H. J. Wang, G. M. Xiang, R. Z. Gong, X. Z. Wei and Z. S. Liu (2015). Unsteady simulation and analysis for hump characteristics of a pump turbine model. *Renewable Energy 77*, 32–42.

Li, D. Y., R. Z. Gong, H. J. Wang, G. M. Xiang, X. Z. Wei and Z. S. Liu (2015). Dynamic analysis on pressure fluctuation in vaneless region of a pump turbine. *Science China Technological Sciences 58*(5), 813–824.

Li, D. Y., R. Z. Gong, H. J. Wang, W. W. Fu, X. Z. Wei and Z. S. Liu (2015). Fluid flow analysis of drooping phenomena in pump mode for a given guide vane setting of a pump-turbine model. *Journal of Zhejiang University Science 11*.

Li, Z., D. Wu, L. Wang and B. Huang (2010). Numerical simulation of the transient flow in a centrifugal pump during starting period. *Journal of Fluids Engineering 132*(8).

Liu, J. T., Y. Wu and Y. Li (2016). Numerical predictions of pressure fluctuations in a model pump turbine with small guide vane opening based on partial averaged navier stokes approach. *Journal of Applied Fluid Mechanics 9*(6), 2661–2669.

Qian, Y. and C. Arakawa (2010). The analysis of rotor-stator interaction phenomena in a pump-turbine. *Energy and Water: Sustainable Development* 302–307.

Ran, H., X. Luo, Z. Lei, Z. Yao, W. Xin and H. Xu (2012). Experimental study of the pressure fluctuations in a pump turbine at large partial flow conditions. Chinese Journal of Mechanical Engineering 25(6), 1205–1209.

Rodriguez, C. G. (2jm007). Frequencies in the vibration induced by the rotor stator interaction in a centrifugal pump turbine. Transactions of Asme *Journal of Fluids Engineering 129*(11), 1428–1435.

Sun, Y. K., Z. G. Zuo, S. H. Liu, J. T. Liu and Y. L. Wu (2012). Numerical study of pressure fluctuations in different guide vanes' opening angle in pump mode of a pump turbine. In *IOP Conference Series: Earth and Environmental Science*.

Tanaka, H. (2011). Vibration behavior and dynamic stress of runners of very high head reversible pump-turbines. *International Journal of Fluid Machinery and Systems 4*, 289–306.

Thanapandi, P. and R. Prasad (1995). Centrifugal pump transient characteristics and analysis using the method of characteristics. *International Journal of Mechanical Sciences 37*(1), 77–89.

Trivedi, C., B. Gandhi and C. J. Michel (2013). Effect of transients on francis turbine runner life: a review. *Journal of Hydraulic Research 51*(2), 121–132.

Wang, H. J., Y. Gao, D. Li, R. G., X. Wei, D. Qin, L. Ming and W. Nie (2015). Analysis of pressure fluctuation of pump-turbine in pump mode based on dynamic mesh. *Large Electric Machine and Hydraulic Turbine* (5).

Wilcox, D. C. (2006). Turbulence modeling for cfd. Dcw Industries La Canada California Usa, 363–367.

Wu, D., P. Wu, Z. Li and L. Wang (2010). The transient flow in a centrifugal pump during the discharge valve rapid opening process. Nuclear Engineering and Design 240(12), 4061 – 4068. *The 6th Japan-Korea Symposium on Nuclear Thermal Hydraulics and Safety-{NTHAS6} Special Section.*

Yin, J. L. (2011). Prediction of pressure fluctuations of pump turbine under off-design condition in pump mode. *Journal of Engineering Thermophysics 32*(7), 1141–1144.

Zobeiri, A., J. L. Kueny, M. Farhat and F. Avellan (2006). Pump-Turbine Rotor-Stator Interactions in Generating Mode: Pressure Fluctuation in Distributor Channel. In 23rd *IAHR Symposium on Hydraulic Machinery and Systems, Number 235.* Hydrodyna.